Algal Research 73 (2023) 103161

Contents lists available at ScienceDirect

Algal Research

journal homepage: www.elsevier.com/locate/algal

Polyphosphate synthesis is an evolutionarily ancient phosphorus storage strategy in microalgae

Alex Cliff [a], Benoit Guieysse [a], Nicola Brown [a], Peter Lockhart [b], Eric Dubreucq [c], Maxence Plouviez [a,*]

[a] School of Food and Advanced Technology, Massey University, Palmerston North, New Zealand
[b] School of Fundamental Sciences, Massey University, Palmerston North, New Zealand
[c] UMR IATE, Institut Agro, INRAE, Montpellier, France

ARTICLE INFO

Keywords:
Polyphosphate
Chlamydomonas
Phylogeny
VTC4
Protein models
Protein homology
AlphaFold

ABSTRACT

To assess the ubiquity of the potential for inorganic polyphosphate (polyP) synthesis in microalgae, we searched databases for algal homologues to the polyP polymerase VTC4 of *Chlamydomonas reinhardtii*. Homologues of this protein were found within >40 species of microalgae known to inhabit marine, freshwater, and terrestrial environments. Phylogenetic analysis demonstrated that these proteins were organized into clades aligning with their taxonomic relationships. These similarities and evolutionary relationships suggest that polyP synthesis represents an ancient ability that has evolved with species as the microalgal lineage has spread out over time. Based on these results and prior knowledge on P metabolism, *C. reinhardtii*, *Chlorella vulgaris*, *Desmodesmus* cf. *armatus*, *Gonium pectorale*, and *Microcystis aeruginosa* were further tested in bioassays known to trigger the synthesis of polyP within dense granules, by addition of P following a period of P depletion. While the cellular P content of *C. reinhardtii*, *G. pectorale*, *M. aeruginosa*, and *D.* cf. *armatus* increased to similar maxima, ranging from 2.6 ± 0.5 % to 3.6 ± 1.3 % 24 h after P repletion, P content only reached 1.2 ± 0.2 % in *C. vulgaris*, suggesting a lesser ability to accumulate polyP than the strains of the other species. Models of predicted VTC4 proteins were generated from the four eukaryotic species tested and showed that the microalgae share the conserved VTC catalytic core and SPX phosphate-sensing domains found in the yeast VTC4 proteins. This confirms the role of microalgal VTC4 as polyP polymerase and suggests a similar regulation of VTC4 proteins to the one described in yeast. Further work is now needed to uncover the assembly of the microalgal VTC complex and its regulation. A deeper study of the microalgal VTC structure could also help to understand whether differences in VTC structures can explain observed differences in P accumulation kinetics.

1. Introduction

In 'The paradox of the plankton', G. E. Hutchinson [1] raised the question of why so much species diversity is observed within natural environments where a relatively homogeneous niche should favour the best-suited species. Responses to changes in availability of the growth-limiting nitrogen and phosphorus sources, may help us to understand the role of these nutrients in giving rise to species diversity.

In microalgae, P is primarily accumulated as polyphosphates (polyP) found in specialized acidocalcisome-like vacuoles [2]. Within these vacuoles, polyP is found as electron-dense granules, originally described in yeast as 'volutin' [3] and colocalized with high concentrations of mono- and divalent cations [4,5]. The role of the membrane-bound vacuolar transporter chaperone (VTC) complex in polyP metabolism has been shown in the yeast *Saccharomyces cerevisiae*. The synthesis of vacuolar polyP is catalyzed by components of the VTC complex using ATP as substrate and is concurrent with its translocation across the vacuole membrane [4,6]. The complex comprises the polyP polymerase VTC4 and location-specific combinations of the accessory VTC1, VTC2, VTC3, and VTC5 subunits [7–9]. The VTC4 protein contains three conserved functional domains: (i) an N-terminal SPX domain (PFAM accession PF03105) involved in P sensing and shown to control VTC activity in yeast [9–12], (ii) a catalytic tunnel domain (also referred as triphosphate tunnel metalloenzyme domain, PFAM accession PF09359) which polymerizes polyP, and (iii) a transmembrane domain (PFAM accession PF02656) which anchors the complex to the vacuolar

* Corresponding author.
E-mail address: M.Plouviez@massey.ac.nz (M. Plouviez).

https://doi.org/10.1016/j.algal.2023.103161
Received 23 February 2023; Received in revised form 22 May 2023; Accepted 26 May 2023
Available online 31 May 2023

membrane and enables translocation of polyP into the vacuole [9,13].

The genome of the model alga *Chlamydomonas reinhardtii* also encodes a VTC4 protein (CrVTC4), homologous to the yeast VTC4, which is required for polyP synthesis [14,15]. To date, little has been revealed about the prevalence of VTC proteins within microalgae and whether putative VTC proteins in other algal species have the same function as the VTC4 found in *C. reinhardtii*, although a search of the literature revealed that >100 unique algal species can synthesize polyP (Table S1).

In this work, we studied the phylogeny of microalgal VTC4 proteins and investigated species differences in polyP synthesis kinetics in microalgae harboring the VTC complex. As no crystal structures of the microalgal VTC proteins were available prior to this study, we used protein homology and the neural network-based AlphaFold structure prediction model [16] to generate the microalgal VTC4 protein subunit models.

2. Methodology

2.1. VTC4 protein homology search

Algal species containing protein sequences homologous to the sequence of the CrVTC4 (Phytozome accession *Cre09.g402775*, GenBank: XP_042921434.1), the polyP polymerase subunit of the *C. reinhardtii* VTC complex were identified using the Basic Local Alignment Search Tool (BLAST) [17] within the NCBI non-redundant protein database. Sequences were aligned using MUSCLE [18]. Conserved blocks of amino acids (298 residues) in the MUSCLE alignment were identified by GBlocks ver. 0.91b (http://phylogeny.lirmm.fr/phylo_cgi/one_task.cgi?task_type=gblocks; default settings used) and used for tree building. A Maximum likelihood tree was constructed using PhyML [19]. Tree building parameters were: BioNJ starting tree, WAG substitution model, NNI rearrangements, site heterogeneity modelled using a discrete gamma distribution with estimated alpha shape parameter, 100 nonparametric bootstrap replicates (values >90/100 shown on the tree).

2.2. Strains and cultivation conditions

Five species of microalgae were selected based on existing knowledge surrounding their P metabolism (Table 1). The *Desmodesmus* cf. *armatus* strain was isolated from a wastewater stabilization pond (WSP) sample and identified from RNAseq data (discussed below) based on 18S ribosomal RNA sequences.

The selected microalgal strains were cultivated on low-phosphorus (1 mg·L^{-1} P) minimal medium (7.48 mM $NaNO_3$; 0.41 mM $MgSO_4{\cdot}7H_2O$; 0.34 mM $CaCl_2{\cdot}2H_2O$; 21.1 μM K_2HPO_4; 10.8 μM KH_2PO_4; Hutner's trace elements, as described by Hill, and Kafer [25], at 1 mL/L final volume), in 250 mL Erlenmeyer (E-) flasks plugged with cotton wool, under continuous illumination at 29 μmol photons·m^{-2}·s^{-1} provided by six 18 W Gro-Lux fluorescent tubes (Sylvania, Wilmington, MA). Temperature was maintained at 25 °C, the air inside the incubator was maintained at 1 % (*v*/v) CO_2, and mixing was done by continuous orbital agitation at 165 min^{-1} in a Minitron incubator (Infors, Bottmingen, Switzerland). Cultures were reinoculated on the same medium, at a ratio of 15–25 mL culture to 100 mL medium, in 250 mL E-flasks, after five days growth.

Table 1
Microalgal species selected for polyP synthesis characterization.

Species (strain)	Order	Relevance to the present work
Chlamydomonas reinhardtii (CC-1690)	Chlamydomonadales	Model organism [20]. Genome fully sequenced [21].
Chlorella vulgaris (UTEX 259)	Chlorellales	Well-studied polyP metabolism [22].
Desmodesmus cf. *armatus*	Sphaeropleales	Isolated from a New Zealand WSP.
Gonium pectorale (UTEX 2582)	Chlamydomonadales	PolyP ability unknown but closely related to *C. reinhardtii*.
Microcystis aeruginosa[a] (UTEX 2385)	Chroococcales	Prevalent in algal blooms [23].

[a] The cyanobacterium *Microcystis aeruginosa*, employs a different regulatory network for maintaining P homeostasis, including the polyP polymerases, PPK1 and PPK2 [24], found primarily in prokaryotic organisms.

2.3. PolyP synthesis and accumulation in five species of microalgae

Cultures were cultivated as described above for five days. After this time, 25 mL was taken from each replicate for initial measurements.

Three of the replicate cultures, designated treatments, were supplied with a phosphate dose equivalent to a final concentration of 10 mg P·L^{-1}, using a 1 M stock solution of phosphate (46 g·L^{-1} KH_2PO_4 and 115 g·L^{-1} K_2HPO_4). The remaining samples, designated controls, were unaltered. Additional 10 mL samples were taken one and five hours after the P addition for initial measurements and cytological staining (as described below). Final 25 mL samples were taken 24 h after P addition and the same methods were applied as with the initial samples.

Optical density (*OD*) was determined at 683 nm using a UV-1800 spectrophotometer (Shimadzu, Kyoto, Japan). Dry weight (*DW*) was determined by filtering 5 mL of sample through a pre-weighed 47 mm glass-fibre filter (1.2 μm), drying 1h at 105 °C, and reweighing. These measurements were performed in triplicate. Extracellular phosphate-P (P_{ext}) was measured by ion chromatography [26]. Total phosphorus (P_{tot}) was quantified colorimetrically, using Hach TNT843 low-range (0.5–1.5 mg·L^{-1} P) test tube kits and a DR3900 spectrophotometer (Hach, Loveland, CO). PolyP granules were stained using the lead sulfide procedure of Bolier et al. [27]. For each sample, 300 μL of culture was pipetted onto a glass slide and dried at 105 °C. This was then wetted with a 25 g/L solution of lead nitrate in 5 % nitric acid and left for five minutes. The slide was rinsed off using reverse osmosis purified (RO) water, wetted with 20 % ammonium sulfide, and left for 10 s before rinsing again with RO water. Slides were dried again at 105 °C and examined using a BX53 light microscope (Olympus) at 100× magnification. Images were captured using a XC50 digital camera (Olympus) and cellSens Dimension v. 1.5 software (Olympus).

Cellular phosphorus content was determined using Eq. (1).

$$\text{Cellular P content} = \frac{(P_{tot} - P_{ext})}{DW} \quad (1)$$

where the cellular P content is the P accumulated in the biomass (g P·g DW^{-1}), P_{tot} is the total P (g P·L^{-1}), P_{ext} is the dissolved P in solution (g PO_4^{3-}-P·L^{-1}), and DW is the dry weight (g-DW·L^{-1}).

The experiments were repeated for each species and the data from separate experimental runs have been pooled increasing the total number of biological replicates.

2.4. RNA extraction

Samples of *C. vulgaris* and *D. armatus* (approximately 50 mL) cultures were centrifuged and the cell pellet was stored at −80 °C. Total RNA was extracted using a Plant and Fungi Mini Kit (Macherey-Nagel). The manufacturer's protocol was followed except that the lysis step was performed by resuspending the thawed pellet in lysis buffer, transferring to a tube containing 10–15 zirconia/silica beads (2.3 mm diameter BioSpec no. 11079125), and homogenizing for 60 s at 5000 rpm using a MagNA Lyser bead mill (Roche).

2.5. Transcriptome assembly

Extracted RNA was sequenced using an Illumina NovaSeq 6000 system with NovaSeq S4 flow cell, producing 60–80 million 150 nt paired-end reads per sample. RNA-seq data were uploaded to the public Galaxy server [28] at https://usegalaxy.org for analysis. Contigs (~0.18 to 35 kbp) were assembled using Trinity 2.9.1 [29]. While the paired-

end reads data have been reposited in the Sequence Read Archive (https://www.ncbi.nlm.nih.gov/sra, accession number: PRJNA953789), the assemblies used have been reposited in Zenodo (*C. vulgaris*: https://doi.org/10.5281/zenodo.7954322 and *D. armatus*: https://doi.org/10.5281/zenodo.7954337).

2.6. Protein sequence prediction

Protein sequences were predicted from the contigs using Transdecoder 5.5.0 [30]. Local BLAST databases were created from the candidate protein sequences and searched for homologues of CrVTC4, as described above.

2.7. Protein structure prediction and substrate docking

The amino acid sequences used for the protein structure prediction can be found in Table S2. VTC4 protein sequences for *C. vulgaris* and *D. armatus* were obtained from database searches and sequencing as described above, while online databases supplied the VTC4 sequences for *C. reinhardtii* (Phytozome: Cre09.g402775) and *G. pectorale* (GenBank: KXZ45148.1). The PPK1 (GenBank: CAO90440.1) and PPK2 (GenBank: CAO90273.1) sequences for *M. aeruginosa* were retrieved from Achbergerová and Nahálka [24]. Models of the VTC4 proteins from *C. reinhardtii*, *C. vulgaris*, *D. armatus*, *G. pectorale,* and *M. aeruginosa* were obtained by two approaches: (i) homology modelling based on experimental crystal structures of the VTC catalytic core and SPX protein domains in *S. cerevisiae*, PPK1 in *Escherichia coli* and PPK2 in *Pseudomonas aeruginosa* available in the Protein Data Bank (3G3Q, VTC domain from VTC4; 5IIQ: SPX domain from VTC4; 1XDP: PPK1; 3CZP: PPK2) using the Phyre2 server [31] and (ii) using DeepMind's neural network-based AlphaFold2 structure prediction model [16]. The predicted models were then further refined by structure equilibration and minimization in a TIP3 water box using NAMD v2.14 [32]. Autodock Vina v1.2.0 [33] was used for ligand docking and UCSF ChimeraX v1.5 [34] to visualize and analyze molecular structures and related data. The parameters selected in the script v1.3.0 provided in ChimeraX 1.5 and used to predict the protein structure using Alphafold2 can be found in Appendix S1.

3. Results and discussion

3.1. Phylogeny of algal VTC4 proteins

The NCBI protein database was searched for amino acids sequences homologous to the sequence of *C. reinhardtii* polyP polymerase VTC4. The results from this search were manually purged of sequences not belonging to microalgae and one sequence was rejected due to low similarity, leaving 48 sequences with percentage identity ranging from 38.96 % to 96.82 %. These sequences were aligned using MUSCLE to identify similarities in conserved regions. Inspection of the alignment revealed that several sequences were incomplete due to the absence of one or more of the three conserved functional domains found in the *C. renhardtii* VTC4 protein (i.e., the N-terminal SPX domain, the catalytic tunnel domain, and the transmembrane domain). The amino acids sequence of the SPX domain was absent from the entries for *Guillardia theta* (XP_00582982.1), *Raphidocelis subcapitata* (GBG00374.1), *Ostreobium quekettii* (CAD7705264.1), and *Thalassiosira pseudonana* (XP_002295322.1). The sequence from *T. pseudonana* begins near the C-terminal end of the SPX domain and Blaby-Haas, and Merchant [35] previously noted that this sequence model had been incorrectly truncated. It is however not clear whether this is also the case for *G. theta*, *R. subcapitata*, and *O. quekettii*. VTC4 sequences for *Haematococcus lacustris* (GFH07673.1, GFH26351.1), *Volvox reticuliferus* (GIL87349.1), *Dunaliella salina* (KAF5830825.1), and *G. theta* (as above) were missing the sequence encoding the transmembrane domain and were therefore removed from the alignment (incomplete sequences could bias the assessment of sequence relatedness). The 40 remaining sequences and the sequences of *C. vulgaris* and *D. armatus* were realigned against the *C. reinhardtii* VTC4 protein sequence.

The phylogenetic structure derived from the sequence differences between all the putative VTC4 proteins (Fig. 1) demonstrates consistency with the current taxonomic relationships between these species [36]. VTC4 sequences from *Auxenochlorella protothecoides*, *Micractinium conductrix*, *Volvox reticuliferus*, and *Haematococcus lacustris* appear to represent isoforms originating from a single gene for each species. Species of Chlorellales form two clades, one of which is more closely related to the remaining Chlorophyta sequences than the other clade. The differences between the sequences in these two clades lie primarily in part of the sequence encoding the transmembrane domain.

Among the species identified from the phylogenic analysis, *Phaeodactylum*, *Thalassiosira*, *Nannochloropsis*, *Chlorella*, *Trebouxia*, *Scenedesmus*, and *Chlamydomonas* have been shown to synthesize polyP [37–42] (Table S1). The microalgal species identified in the search are also known to inhabit marine, freshwater, and terrestrial environments, suggesting that the ability to synthesize polyP is not limited to a specific niche. PolyP synthesis has in fact also been observed in eukaryotic microalgae inhabiting arctic regions [43], hot springs [44], and acidic environments [45]. The phylogeny of the putative VTC4 sequences suggests the ability to synthesize polyP has evolved to suit the needs of different species. Together with the presence of putative VTC4 proteins within multiple phyla, this suggests that polyP synthesis is ancient and likely a critical and universal function in microalgae. The polyP-synthesis ability of species from the other genera identified in the BLAST search should now be experimentally verified. Evidence that all species harboring VTC4 gene homologues can synthesize polyP is indeed important to demonstrate that the functionality of the VTC complex has been preserved throughout evolution.

3.2. PolyP synthesis and accumulation in five species of microalgae

C. reinhardtii, *C. vulgaris*, *G. pectorale*, *D. armatus*, and *M. aeruginosa* were cultivated in low-P conditions and subsequently repleted with inorganic phosphate to ascertain their abilities to accumulate P as polyP. Cytological staining confirmed the presence of polyP granules in all the tested microalgae (Fig. S1). PolyP accumulation by *G. pectorale* is reported here for the first time, confirming the ability suggested by the presence of a VTC4 protein homologue.

The cellular phosphorus content (%P) was calculated for each biological replicate and averaged for each species. As can be seen in Fig. 2, all species rapidly accumulated the P supplied and the kinetics of intracellular P accumulation (and related polyP synthesis, Fig. S2) were species-dependent: *M. aeruginosa* and *G. pectorale* exhibited the largest gains in cellular phosphorus content 1 h after P repletion, with P content increasing to 2.7 ± 0.4 % and 2.1 ± 1.2 % of dry biomass, respectively (paired t-test, $p < 0.01$). From 1 to 5 h after P repletion, the cellular phosphorus content increased significantly in all the species tested, with the largest increase from 0.9 ± 0.4 % to 2.9 ± 0.3 % being recorded in *C. reinhardtii* (paired t-test, $p < 0.01$). Between 5 and 24 h after P repletion, the cellular phosphorus content only changed significantly ($p < 0.05$) in *D. armatus* and *M. aeruginosa*, in both cases decreasing. *D. armatus* grew by 40 ± 12 % over this period, which resulted in a decrease of intracellular P relative to dry weight as all the P initially supplied had already been assimilated bv the cells. The cellular P content values recorded ranged from 1.15 % (*C. vulgaris*) to 3.55 % (*G. pectorale*). These values are consistent with values previously reported in the literature (Table 2).

Only *M. aeruginosa* grew significantly more over 24 h in treatment cultures than in control cultures (t-test, $p < 0.05$) whereas the other cultures grew similarly in control and treatment cultures (Fig. S3). The negligible impact of P repletion on growth in those cases indicates that the microalgae were not P-limited for growth under the conditions tested. Since there is no P limitation, we would not expect the cells to be predisposed to assimilate excess P. The ability to accumulate P under

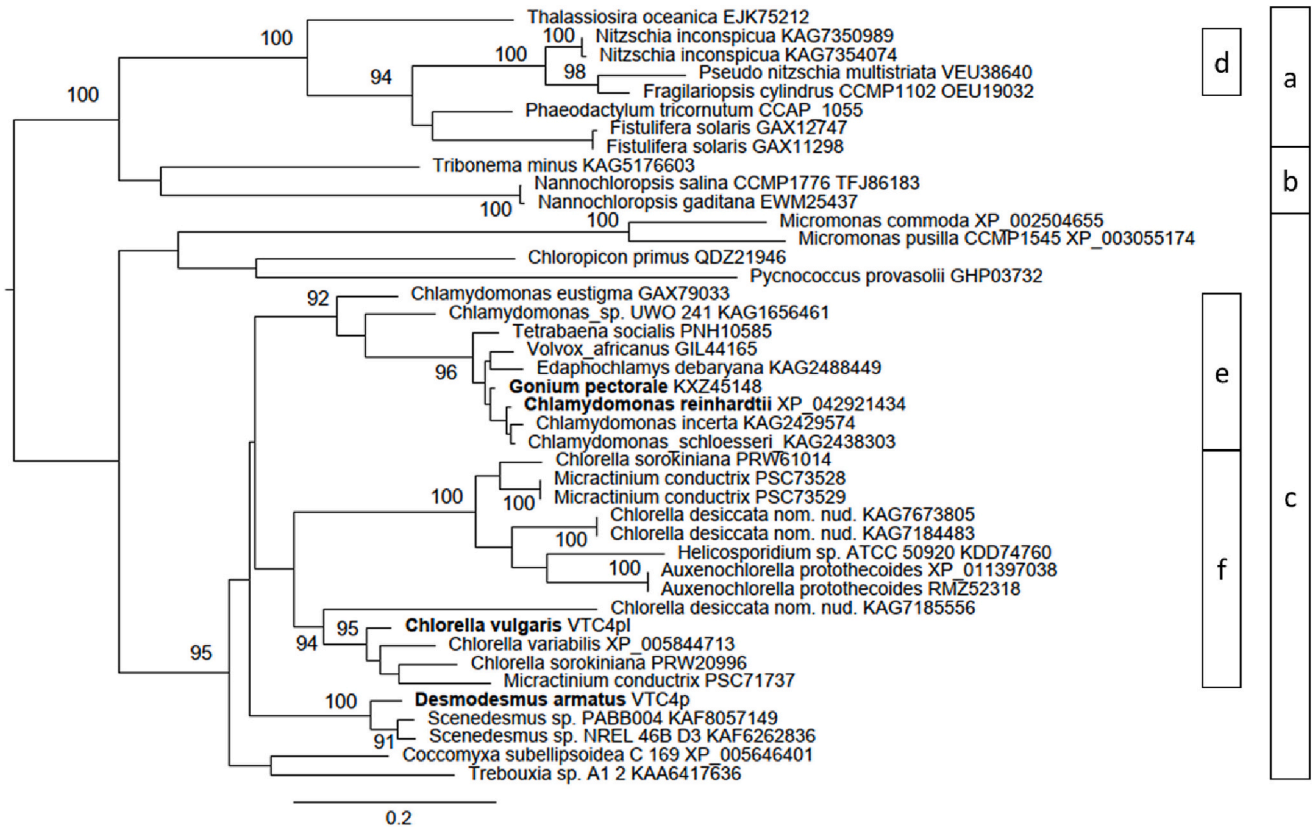

Fig. 1. Cladogram of putative VTC4 protein sequences (accession numbers in parentheses) found through a BLAST search for sequences with similarity to CrVTC4 (Cre09.g402775), showing clades corresponding to groupings by phylum (a: Bacillariophyta; b: Ochrophyta; c: Chlorophyta) and order (d: Bacillariales; e: Chlamydomonadales; f: Chlorellales). Scale for branch lengths (substitutions per site) is shown. No proteins from higher plants were included because higher plants such as *Arabidopsis* do not possess a vacuolar transport chaperone complex acting as polyP polymerase. Besides, higher plants have never been shown to synthesize inorganic polyP granules [46].

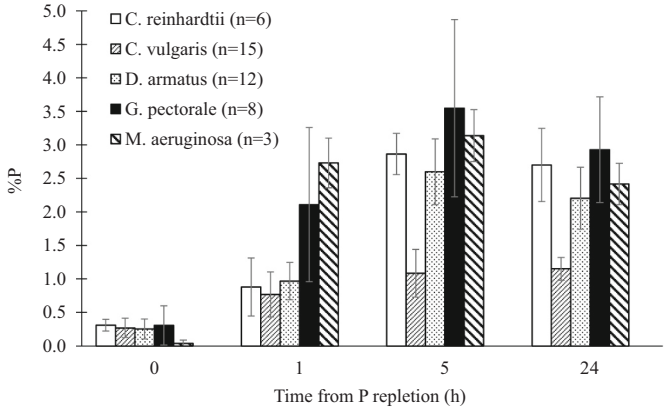

Fig. 2. Cellular P content (%P as the weight fraction of dry biomass) in the five microalgal species examined, at the indicated times following P addition (mean ± standard deviation of *n* biological replicates).

non-limited conditions should however benefit microalgae by prolonging P availability when external P becomes limiting and thereby acts as a survival mechanism under intermittent P supply. Since growth did not slow when polyP was formed (i.e., in treatment cultures), the energy cost of polyP synthesis must be negligible compared to the costs of biomass growth. This was demonstrated with simple energy calculations by Plouviez et al. [52] who therefore concluded that polyP is a P reserve rather than an energy source in microalgae.

Table 2
Maximum cellular P content (%P_{max}, as weight fraction of dry biomass) values reported in the literature and in this study (mean ± standard deviation). WSP = waste stabilization ponds.

Study	%P_{max} (%)	Community profile
Powell et al. [47]	3.16	Mixed culture dominated by *Scenedesmus* spp.
Powell et al. [48]	3.85	WSP sample
Schmidt, Gagnon, and Jamieson [49]	3.30	Mixed culture of *Chlamydomonas reinhardtii* and *Chlorella vulgaris*
Crimp, Brown, and Shilton [50]	3.80	WSP sample
Solovchenko et al. [51]	5.00	*C. vulgaris* and *Parachlorella kessleri*
Plouviez et al. [14]	2.64	*C. reinhardtii*
This study	2.90 ± 0.30	*C. reinhardtii*
This study	1.20 ± 0.20	*C. vulgaris*
This study	2.60 ± 0.50	*Desmodesmus* cf. *armatus*
This study	3.60 ± 1.30	*Gonium pectorale*
This study	3.10 ± 0.40	*Microcystis aeruginosa*

3.3. Protein structure prediction and substrate docking

While the involvement of VTC proteins in polyP synthesis has been demonstrated in *C. reinhardtii* [14,53,54], this function in the other microalgae herein tested was only inferred based on protein homology

using BLAST searches and sequence alignments [55].

To assess the polyP polymerase activity of VTC complexes from these microalgae, the first 3D structures of key VTC4 protein domains (i.e., the VTC polyP polymerase catalytic core and the SPX phosphate sensor domain) from *C. reinhardtii*, *C. vulgaris, D. armatus*, and *G. pectorale* were predicted based on the VTC4 amino acid sequences (see an example in Fig. 3). Pairwise similarity between the amino acid sequences was higher between the microalgae than with the yeast (Table S3).

Structure prediction was performed by homology modelling using a classical template-based approach and using the Alphafold2 neural network-based model, followed by molecular dynamics structure equilibration and energy minimization in the presence of a docked polyP (5 residues) in a water box at 25 °C. Due to the high structural homology between the microalgal proteins sequences to *S. cerevisiae* protein sequence (38–44 % sequence identity with ~60 % sequence coverage including the VTC catalytic core), both approaches yielded very close predicted structures except in unstructured outer loops. Considering the advances brought by the recent deep-learning approach, and for consistency, only the structures predicted by AlphaFold2 were finally retained for this study. As can be seen in Fig. 4, the four predicted microalgal VTC4 structures share a fair structural homology with the VTC4 protein from *S. cerevisiae.* By contrast, the cyanobacterial polyphosphate kinases (PPK1 and PPK2), known to catalyse polyP in prokaryotes [24], were structurally different to the VTC structures (only 18 % sequence identity on 28 aligned residues and 16 % identity on 19 aligned residues, for PPK1 and PPK2, respectively, versus *S. cerevisiae* VTC4).

The level of protein sequence homology between microalgal VTCs and yeast (Table S3) allows reasonable confidence in the structure prediction of the VTC catalytic core and SPX domains in the microalgae. Furthermore, docking calculations using a $polyP_5$ model showed a similar positioning of the $polyP_5$ chain within the catalytic sites (Fig. 4), in agreement with the experimental evidence of the polyP catalytic role of the VTC complex in *C. reinhardtii* [14].

The structural similarities for the predicted VTC4 proteins of *C. vulgaris*, *D. armatus* and *G. pectorale*, identified by sequence homology, indicate that these sequences indeed encode VTC4 proteins with similar functionality to the VTC4 of *C. reinhardtii*.

To the best of our knowledge, the models presented in Fig. 4 are the first microalgal VTC protein models currently described. Critically, the predicted structure of VTC4 is confirmed to be compatible with a polyP polymerase function in *C. reinhardtii*, *C. vulgaris*, *D. armatus,* and *G. pectorale*. In addition, the structural similarity of the SPX domains and the positioning of inositol hexakisphosphate ($InsP_6$) calculated by

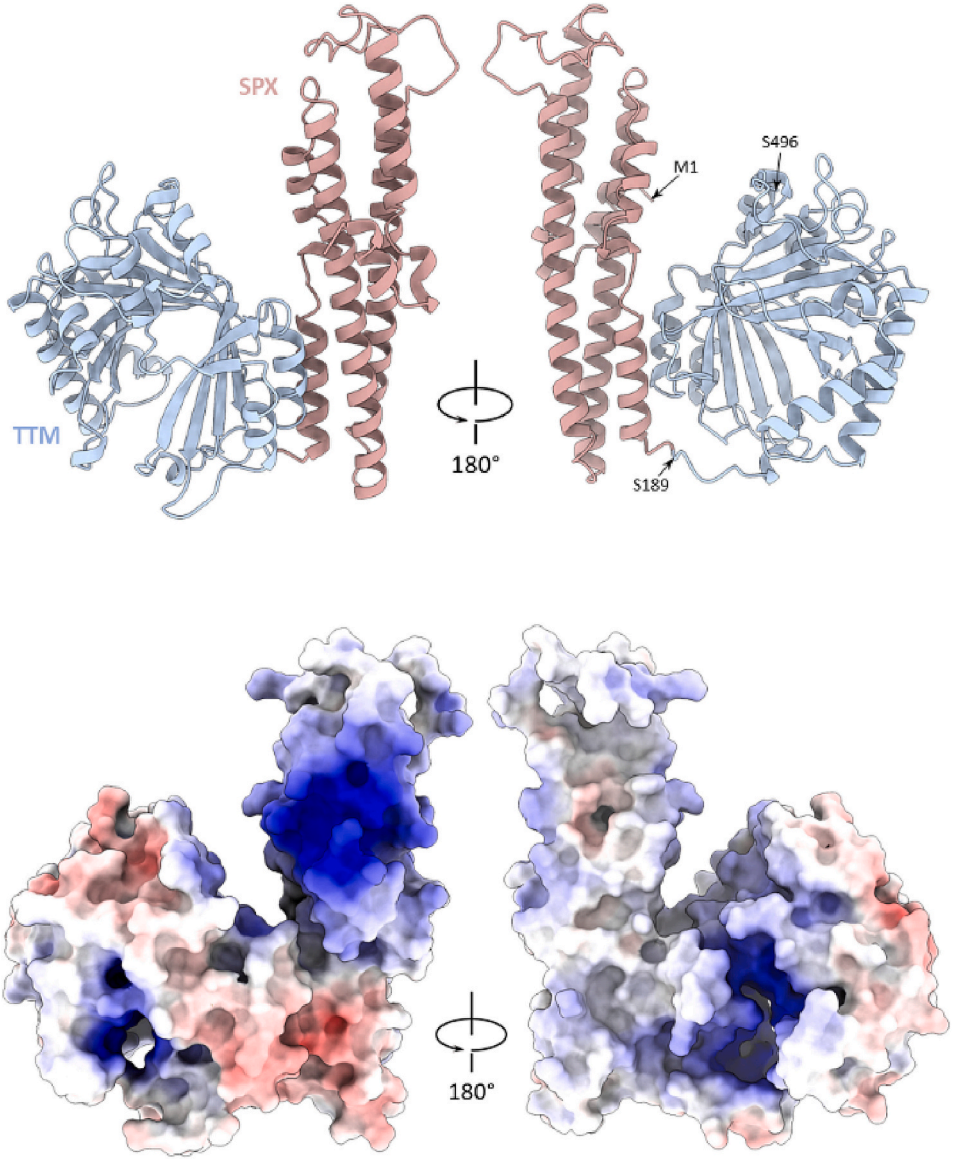

Fig. 3. *Top:* Two-side views (180° rotation) of the *Gonium pectorale* VTC4 protein structure generated using AlphaFold2: Cartoon model showing the SPX (plum colour, from Methionine M1 to Aspartic acid D188) and the catalytic tunnel domain (TTM, in blue, from Serine S189 to Serine S496) linked domains. *Bottom:* Surface model (in the same perspective as the cartoon model), colored according to the surface electrostatic potential (red: negative; blue: positive). (For interpretation of the references to colour in this figure legend, the reader is referred to the web version of this article.)

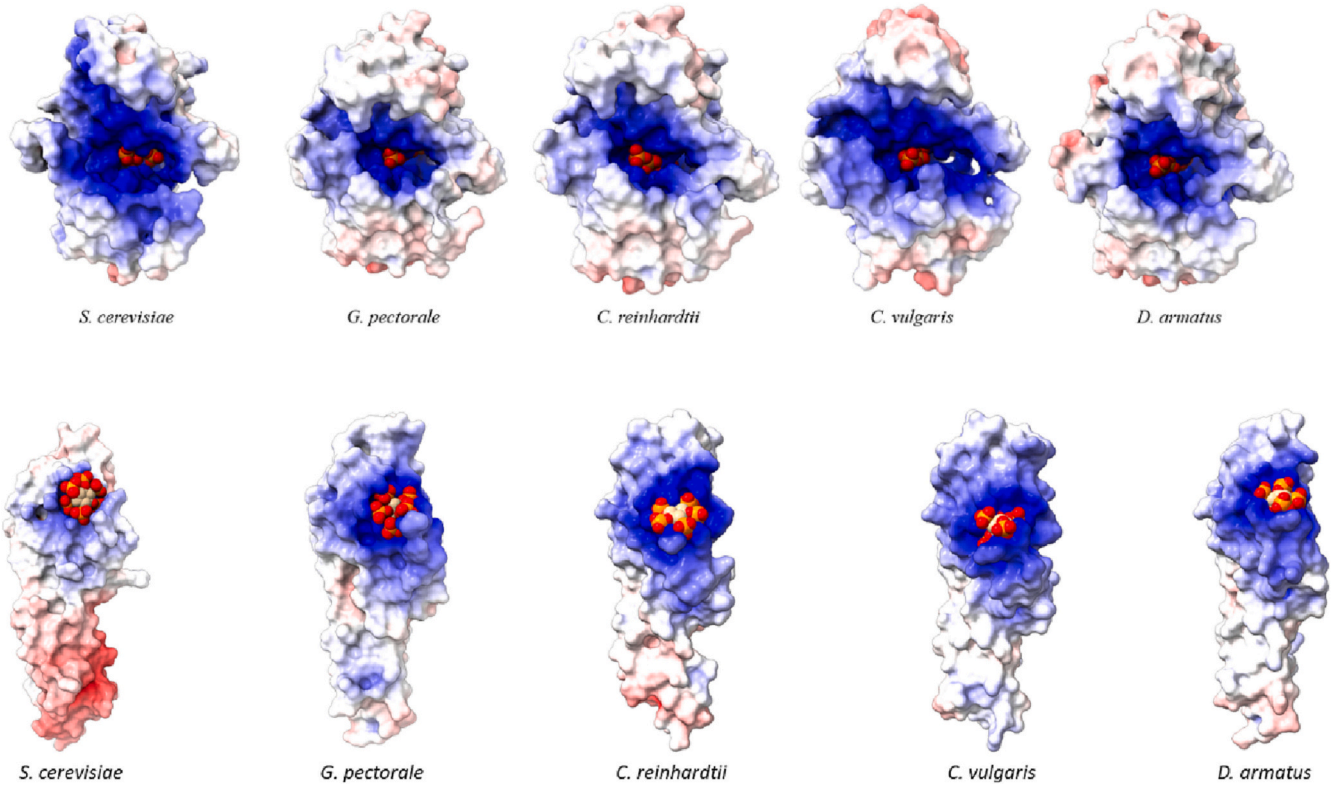

Fig. 4. VTC4 structural models for *G. pectorale*, *C. reinhardtii*, *C. vulgaris* and *D. armatus,* compared to the experimentally derived *S. cerevisiae* protein structure. Surface colours are mapped to the electrostatic potential (−10: red to 10: blue KbT/e) at pH 7.0 of the apo form. Top: The VTC catalytic core domain, shown in complex with a $polyP_5$ molecule. Cartoon representations of the *S. cerevisiae* and *G. pectorale* models can be found in Fig. S4. Bottom: The SPX domain in complex with an inositol hexakisphosphate ($InsP_6$) molecule. The cyanobacterial PPK1 and PPK2 models can be found in Fig. S5. (For interpretation of the references to colour in this figure legend, the reader is referred to the web version of this article.)

docking calculations using an $InsP_6$ model (Fig. 4) suggests that the microalgal VTC4 proteins could be regulated via binding of inositol pyrophosphates to the SPX domain as proposed by Plouviez et al. [14].

Notably, Guan et al. [9] recently analysed the structure of the *S. cerevisiae* (strain BY4741) VTC1/3/4 vacuolar sub-complex (a pentamer in a 3:1:1 stochiometric ratio), using cryo-electron microscopy. It was shown that VTC3 and VTC4 contain transmembrane domains that combined with VTC1 to form the transmembrane channel. Both VTC3 and VTC4 have triphosphate tunnel metalloenzyme (TTM) domains but the VTC4 TTM domain is the one responsible for synthesizing polyP. PolyP synthesis is activated via binding of inositol phosphates such as InsP6 to VTC3 and VTC4 SPX sensory domains. When activated, the VTC4 TTM tunnel moves close to the transmembrane region most likely facilitating the transport of the newly made polyP chain from the VTC4 tunnel towards the transmembrane channel. To the best of our knowledge, microalgae only possess homologues of the VTC1 and VTC4 subunits of *S. cerevisae*, meaning that the structure of the microalgal VTC complex could be different to the structure of the yeast VTC. Further work is now needed to uncover how the microalgal VTC complex is assembled and activated. Besides, studying VTC structures could explain the differences in polyP accumulation abilities reported among microalgae species (Table 2) and to unravel how polyP synthesis is regulated at the protein level. Production of these enzymes by heterologous expression and subsequent in vitro characterization may reveal whether the action of these proteins is reversible, as it has recently been shown to be in fungal VTC4 proteins [56].

3.4. Ecological and environmental implications

Plouviez et al. [57] previously suggested a common evolution of P metabolism (including polyP synthesis) in microalgae. This is supported by our study showing that microalgae found in different ecological niches are able to synthesize polyP and that VTC4 is broadly conserved. Algae have therefore evolved to be particularly efficient at harvesting P as intracellular polyP, an ability that could be harnessed to mitigate water pollution. However, considerable advances are still needed in our fundamental understanding of P-metabolism in algae before P-upcycling can be engineered by triggering polyP synthesis on-demand [58]. To the best of our knowledge, while parameters such as light intensity, temperature, and N:P ratio have been shown to influence P accumulation in microalgae during wastewater treatment [47,59,60], the influence of these parameters on specific P-related genes and proteins (including polyP polymerases) is currently unknown. Our previous data [14,57,61] indicated that differences in the regulation of the genes involved in synthesizing polyP are insufficient to explain the differences in polyP synthesis yields and kinetics in *Chlamydomonas*. We therefore believe that the synthesis of polyP is regulated at the protein level in microalgae, similarly to other organisms such as yeast. In yeast, polyP polymerase proteins are regulated by interactions with inositol pyrophosphates [62]. The data presented in Fig. 4 would suggest that regulation of polyP synthesis could also occur via binding of inositol pyrophosphate in microalgae. Further research is needed to confirm this finding and to determine if difference in VTC efficiency (or regulation) could explain inter-species differences in their capacity for polyP accumulation. With continual improvements in computational capacity, *insilico* modelling could therefore be used as a screening tool for differentiating microalgal polyP synthesizing ability and providing insight into the use of the "best" microalgae to test to ultimately develop microalgae-based technologies for P removal via polyP synthesis.

4. Conclusions

A BLAST search for protein homologues of the *C. reinhardtii* polyP polymerase CrVTC4 revealed similar protein sequences in 48 species of microalgae distributed across 3 phyla. Phylogenetic analysis demonstrated that the proteins are organized into clades aligning with their taxonomic relationships. These similarities and evolutionary relationships suggest that the *vtc4* gene is ancient and has evolved with species over time. Therefore, it is likely that this gene is present within most eukaryotic microalgae and that the ability to synthesize polyP is conserved and critical. This in turn suggests that microalgal polyP synthesis takes place in all environments where microalgae are found.

For the first time, five species (including four species known to possess putative VTC4 proteins and one possessing PPK proteins) were assayed under similar conditions for their ability to assimilate P and accumulate polyP upon P repletion following a period of P depletion. All strains accumulated polyP as granules but *C. vulgaris* assimilated less P than the other species. For most species, growth was not negatively affected by P assimilation and polyP synthesis, confirming that the energy cost of polyP synthesis does not affect growth.

The first microalgal VTC4 models were presented and showed structural conservation of the VTC catalytic site and SPX domain, confirming that the structures of CrVTC4 and the predicted VTC4 proteins of *C. vulgaris*, *D. armatus* and *G. pectorale* are compatible with polyP-polymerase activity with potential activation via the SPX domain. Further work is now needed to uncover the assembly of the microalgal VTC complex and its regulation. A deeper study of the microalgal VTC structure could also help to understand whether differences in VTC structure observed can explain the differences in P accumulation kinetics observed in the bioassays. This knowledge could provide insight into the use of the "best" microalgae to test to ultimately develop microalgae-based technologies for P removal via polyP synthesis.

Declaration of competing interest

The authors declare that they have no known competing financial interests or personal relationships that could have appeared to influence the work reported in this paper.

Data availability

Data will be made available on request.

Acknowledgments

This research was supported by Massey University (Strategic Research Excellence Fund), the Marsden Fund Council from New Zealand government funding, administrated by the Royal Society of New Zealand (grant MAU1711) and the embassy of France in New Zealand (F2RP project).

Appendix A. Supplementary data

Supplementary data to this article can be found online at https://doi.org/10.1016/j.algal.2023.103161.

References

[1] G.E. Hutchinson, The paradox of the plankton, Am. Nat. 95 (882) (1961) 137–145, https://doi.org/10.1086/282171.a.
[2] F.A. Ruiz, N. Marchesini, M. Seufferheld, Govindjee, R. Docampo, The polyphosphate bodies of *Chlamydomonas reinhardtii* possess a proton-pumping pyrophosphatase and are similar to acidocalcisomes, J. Biol. Chem. 276 (49) (2001) 46196–46203, https://doi.org/10.1074/jbc.M105268200.
[3] L. Nagel, Volutin, Bot. Rev. 14 (3) (1948) 174–184, https://doi.org/10.1007/BF02861553.
[4] M. Tsednee, et al., Manganese co-localizes with calcium and phosphorus in *Chlamydomonas* acidocalcisomes and is mobilized in manganese-deficient conditions, J. Biol. Chem. 294 (46) (2019) 17626–17641, https://doi.org/10.1074/jbc.RA119.009130.
[5] S.P. Slocombe, T. Zúñiga-Burgos, L. Chu, N.J. Wood, M.A. Camargo-Valero, A. Baker, Fixing the broken phosphorus cycle: wastewater remediation by microalgal polyphosphates, Front. Plant Sci. 11 (2020), https://doi.org/10.3389/fpls.2020.00982.
[6] R. Gerasimaitė, S. Sharma, Y. Desfougères, A. Schmidt, A. Mayer, Coupled synthesis and translocation restrains polyphosphate to acidocalcisome-like vacuoles and prevents its toxicity, J. Cell Sci. 127 (23) (2014) 5093, https://doi.org/10.1242/jcs.159772.
[7] Y. Desfougeres, R. Gerasimaite, H.J. Jessen, A. Mayer, Vtc5, a novel subunit of the vacuolar transporter chaperone complex, regulates polyphosphate synthesis and phosphate homeostasis in yeast, J. Biol. Chem. 291 (42) (2016) 22262–22275, https://doi.org/10.1074/jbc.M116.746784.
[8] M. Hothorn, et al., Catalytic core of a membrane-associated eukaryotic polyphosphate polymerase, Science. 324 (5926) (2009) 513–516, https://doi.org/10.1126/science.1168120.
[9] Z. Guan, et al., The cytoplasmic synthesis and coupled membrane translocation of eukaryotic polyphosphate by signal-activated VTC complex, Nat. Commun. 14 (1) (2023) 718, https://doi.org/10.1038/s41467-023-36466-4.
[10] H.C. Hürlimann, B. Pinson, M. Stadler-Waibel, S.C. Zeeman, F.M. Freimoser, The SPX domain of the yeast low-affinity phosphate transporter Pho90 regulates transport activity, EMBO Rep. 10 (9) (2009) 1003–1008, https://doi.org/10.1038/embor.2009.105.
[11] D. Secco, et al., The emerging importance of the SPX domain-containing proteins in phosphate homeostasis, New Phytol. 193 (4) (2012) 842–851, https://doi.org/10.1111/j.1469-8137.2011.04002.x.
[12] Z. Guan, et al., Mechanistic insights into the regulation of plant phosphate homeostasis by the rice SPX2 – PHR2 complex, Nat. Commun. 13 (1) (2022) 1581, https://doi.org/10.1038/s41467-022-29275-8.
[13] R. Gerasimaitė, A. Mayer, Enzymes of yeast polyphosphate metabolism: structure, enzymology and biological roles, Biochem. Soc. Trans. 44 (1) (2016) 234, https://doi.org/10.1042/BST20150213.
[14] M. Plouviez, et al., Responses of *Chlamydomonas reinhardtii* during the transition from P-deficient to P-sufficient growth (the P-overplus response): the roles of the vacuolar transport chaperones and polyphosphate synthesis, J. Phycol. 57 (3) (2021), https://doi.org/10.1111/jpy.13145.
[15] E. Sanz-Luque, D. Bhaya, A.R. Grossman, Polyphosphate: a multifunctional metabolite in cyanobacteria and algae. *Frontiers*, Plant Sci. 11 (938) (2020), https://doi.org/10.3389/fpls.2020.00938.
[16] J. Jumper, et al., Highly accurate protein structure prediction with AlphaFold, Nature 596 (7873) (2021) 583–589, https://doi.org/10.1038/s41586-021-03819-2.
[17] S.F. Altschul, W. Gish, W. Miller, E.W. Myers, D.J. Lipman, Basic local alignment search tool, J. Mol. Biol. 215 (3) (1990) 403–410, https://doi.org/10.1016/S0022-2836(05)80360-2.
[18] R.C. Edgar, MUSCLE: multiple sequence alignment with high accuracy and high throughput, Nucleic Acids Res. 32 (5) (2004) 1792–1797, https://doi.org/10.1093/nar/gkh340.
[19] S. Guindon, J.-F. Dufayard, V. Lefort, M. Anisimova, W. Hordijk, O. Gascuel, New algorithms and methods to estimate maximum-likelihood phylogenies: assessing the performance of PhyML 3.0, Syst. Biol. 59 (3) (2010) 307–321, https://doi.org/10.1093/sysbio/syq010.
[20] E.H. Harris, *Chlamydomonas* as a model organism, Annu. Rev. Plant Physiol. Plant Mol. Biol. 52 (1) (2001) 363–406, https://doi.org/10.1146/annurev.arplant.52.1.363.
[21] S.S. Merchant, et al., The *Chlamydomonas* genome reveals the evolution of key animal and plant functions, Science. 318 (5848) (2007) 245–250, https://doi.org/10.1126/science.1143609.
[22] P.A. Aitchison, V.S. Butt, The relation between the synthesis of inorganic polyphosphate and phosphate uptake by *Chlorella vulgaris*, J. Exp. Bot. 24 (3) (1973) 497–510, https://doi.org/10.1093/jxb/24.3.497.
[23] L. Jacobson, M. Halmann, Polyphosphate metabolism in the blue-green alga *Microcystis aeruginosa*, J. Plankton Res. 4 (3) (1982) 481–488, https://doi.org/10.1093/plankt/4.3.481.
[24] L. Achbergerová, J. Nahálka, PPK1 and PPK2 — which polyphosphate kinase is older? Biologia. 69 (3) (2014) 263–269, https://doi.org/10.2478/s11756-013-0324-x.
[25] T.W. Hill, E. Kafer, Improved protocols for Aspergillus minimal medium: trace element and minimal medium salt stock solutions, Fungal Genet. Rep. 48 (1) (2001) 20–21, https://doi.org/10.4148/1941-4765.1173.
[26] M. Plouviez, A. Shilton, M.A. Packer, B. Guieysse, N_2O emissions during microalgae outdoor cultivation in 50 L column photobioreactors, Algal Res. 26 (2017) 348–353, https://doi.org/10.1016/j.algal.2017.08.008.
[27] G. Bolier, M.C.J. de Koningh, J.C. Schmale, M. Donze, Differential luxury phosphate response of planktonic algae to phosphorus removal, Hydrobiologia 243 (1) (1992) 113–118, https://doi.org/10.1007/bf00007026.
[28] E. Afgan, et al., The Galaxy platform for accessible, reproducible and collaborative biomedical analyses: 2018 update, Nucleic Acids Res. 46 (W1) (2018) W537–W544, https://doi.org/10.1093/nar/gky379.
[29] M.G. Grabherr, et al., Full-length transcriptome assembly from RNA-Seq data without a reference genome, Nat. Biotechnol. 29 (7) (2011) 644–652, https://doi.org/10.1038/nbt.1883.
[30] B.J. Haas, et al., De novo transcript sequence reconstruction from RNA-seq using the trinity platform for reference generation and analysis, Nat. Protoc. 8 (8) (2013) 1494–1512, https://doi.org/10.1038/nprot.2013.084.

[31] L.A. Kelley, S. Mezulis, C.M. Yates, M.N. Wass, M.J. Sternberg, The Phyre2 web portal for protein modeling, prediction and analysis, Nat. Protoc. 10 (6) (2015) 845–858, https://doi.org/10.1038/nprot.2015.053.
[32] J.C. Phillips, et al., Scalable molecular dynamics on CPU and GPU architectures with NAMD, J. Chem. Phys. 153 (4) (2020), 044130, https://doi.org/10.1063/5.0014475.
[33] O. Trott, A.J. Olson, AutoDock Vina: improving the speed and accuracy of docking with a new scoring function, efficient optimization, and multithreading, J. Comput. Chem. 31 (2) (2010) 455–461, https://doi.org/10.1002/jcc.21334.
[34] E.F. Pettersen, et al., UCSF ChimeraX: structure visualization for researchers, educators, and developers, Protein Sci. 30 (1) (2021) 70–82, https://doi.org/10.1002/pro.3943.
[35] C.E. Blaby-Haas, S.S. Merchant, Regulating cellular trace metal economy in algae, Curr. Opin. Plant Biol. 39 (2017) 88–96, https://doi.org/10.1016/j.pbi.2017.06.005.
[36] M.D.G. Guiry, M. G, AlgaeBase, Retrieved from: https://www.algaebase.org, 2022.
[37] J.M. Leitão, B. Lorenz, N. Bachinski, C. Wilhelm, W.E.G. Müller, H.C. Schröder, Osmotic-stress-induced synthesis and degradation of inorganic polyphosphates in the alga *Phaeodactylum tricornutum*, Mar. Ecol. Prog. Ser. 121 (1995) 279–288, https://doi.org/10.3354/meps121279.
[38] S.T. Dyhrman, et al., The transcriptome and proteome of the diatom *Thalassiosira pseudonana* reveal a diverse phosphorus stress response, PLoS One 7 (3) (2012), e33768, https://doi.org/10.1371/journal.pone.0033768.
[39] A. Mühlroth, et al., Mechanisms of phosphorus acquisition and lipid class remodeling under P limitation in a marine microalga, Plant Physiol. 175 (4) (2017) 1543–1559, https://doi.org/10.1104/pp.17.00621.
[40] G.Y. Rhee, A continuous culture study of phosphate uptake, growth rate and polyphosphate in *Scenedesmus* sp, J. Phycol. 9 (4) (1973) 495–506, https://doi.org/10.1111/j.1529-8817.1973.tb04126.x.
[41] K.A. Fisher, Polyphosphate in a chlorococcalean alga, Phycologia. 10 (2–3) (1971) 177–182, https://doi.org/10.2216/i0031-8884-10-2-177.1.
[42] K. Keck, H. Stich, The widespread occurrence of polyphosphate in lower plants, Ann. Bot. 21 (4) (1957) 611–619, https://doi.org/10.1093/oxfordjournals.aob.a083588.
[43] D. Barcytė, J. Pilátová, P. Mojzeš, L. Nedbalová, The arctic *Cylindrocystis* (Zygnematophyceae, Streptophyta) green algae are genetically and morphologically diverse and exhibit effective accumulation of polyphosphate, J. Phycol. 56 (1) (2020) 217–232, https://doi.org/10.1111/jpy.12931.
[44] S. Nagasaka, E. Yoshimura, External iron regulates polyphosphate content in the acidophilic, thermophilic alga *Cyanidium caldarium*, Biol. Trace Elem. Res. 125 (3) (2008) 286, https://doi.org/10.1007/s12011-008-8177-9.
[45] K. Nishikawa, et al., Polyphosphate metabolism in an acidophilic alga *Chlamydomonas acidophila* KT-1 (Chlorophyta) under phosphate stress, Plant Sci. 170 (2) (2006) 307–313, https://doi.org/10.1016/j.plantsci.2005.08.025.
[46] J. Zhu, et al., A genetically validated approach for detecting inorganic polyphosphates in plants, Plant J. 102 (3) (2020) 507–516, https://doi.org/10.1111/tpj.14642.
[47] N. Powell, A.N. Shilton, S. Pratt, Y. Chisti, Factors influencing luxury uptake of phosphorus by microalgae in waste stabilization ponds, Environ. Sci. Technol. 42 (16) (2008) 5958–5962, https://doi.org/10.1021/es703118s.
[48] N. Powell, A. Shilton, S. Pratt, Y. Chisti, Luxury uptake of phosphorus by microalgae in full-scale waste stabilisation ponds, Water Sci. Technol. 63 (4) (2011) 704–709, https://doi.org/10.2166/wst.2011.116.
[49] J.J. Schmidt, G.A. Gagnon, R.C. Jamieson, Microalgae growth and phosphorus uptake in wastewater under simulated cold region conditions, Ecol. Eng. 95 (2016) 588–593, https://doi.org/10.1016/j.ecoleng.2016.06.114.
[50] A. Crimp, N. Brown, A. Shilton, Microalgal luxury uptake of phosphorus in waste stabilization ponds – frequency of occurrence and high performing genera, Water Sci. Technol. 78 (1) (2018) 165–173, https://doi.org/10.1007/s11157-014-9337-3.
[51] A. Solovchenko, et al., Phosphorus starvation and luxury uptake in green microalgae revisited, Algal Res. 43 (2019), 101651, https://doi.org/10.1016/j.algal.2019.101651.
[52] M. Plouviez, C.S. Oliveira da Rocha, B. Guieysse, Intracellular polyphosphate is a P reserve in *Chlamydomonas reinhardtii*, Algal Res. 66 (2022), 102779, https://doi.org/10.1016/j.algal.2022.102779.
[53] M. Aksoy, W. Pootakham, A.R. Grossman, Critical function of a *Chlamydomonas reinhardtii* putative polyphosphate polymerase subunit during nutrient deprivation, Plant Cell 26 (10) (2014) 4214–4229, https://doi.org/10.1105/tpc.114.129270.
[54] E. Sanz-Luque, S. Saroussi, W. Huang, N. Akkawi, A.R. Grossman, Metabolic control of acclimation to nutrient deprivation dependent on polyphosphate synthesis, Sci. Adv. 6 (40) (2020) eabb5351, https://doi.org/10.1126/sciadv.abb5351.
[55] C.E. Blaby-Haas, S.S. Merchant, The ins and outs of algal metal transport, Biochim. Biophys. Acta, Mol. Cell Res. 1823 (9) (2012) 1531–1552, https://doi.org/10.1016/j.bbamcr.2012.04.010.
[56] C.T. Nguyen, T. Ezawa, K. Saito, Polyphosphate polymerizing and depolymerizing activity of VTC4 protein in an arbuscular mycorrhizal fungus, Soil Sci. Plant Nutr. 1-12 (2022), https://doi.org/10.1080/00380768.2022.2029220.
[57] M. Plouviez, M. Abyadeh, M. Hasan, M. Mirzaei, J.A. Paulo, B. Guieysse, The proteome of *Chlamydomonas reinhardtii* during phosphorus depletion and repletion, Algal Res. 71 (2023), 103037, https://doi.org/10.1016/j.algal.2023.103037.
[58] M. Plouviez, P. Bolot, A. Shilton, B. Guieysse, Phosphorus uptake and accumulation in *Chlamydomonas reinhardtii*: influence of biomass concentration, phosphate concentration, phosphorus depletion time, and light supply, Algal Res. 71 (2023), 103085, https://doi.org/10.1016/j.algal.2023.103085.
[59] N. Powell, A. Shilton, Y. Chisti, S. Pratt, Towards a luxury uptake process via microalgae – defining the polyphosphate dynamics, Water Res. 43 (17) (2009) 4207–4213, https://doi.org/10.1016/j.watres.2009.06.011.
[60] A. Lavrinovičs, L. Mežule, T. Juhna, Microalgae starvation for enhanced phosphorus uptake from municipal wastewater, Algal Res. 52 (2020), 102090, https://doi.org/10.1016/j.algal.2020.102090.
[61] A. Cliff, Environmental Influences on Polyphosphate Accumulation in Microalgae: An Investigation into Species Differences and Transcriptional Responses: A Thesis Presented in Partial Fulfilment of the Requirements for the Degree of Doctor of Philosophy in Engineering at Massey University, Manawatū, Massey University, New Zealand, 2022.
[62] C. Azevedo, A. Saiardi, Eukaryotic phosphate homeostasis: the inositol pyrophosphate perspective, Trends Biochem. Sci. 42 (3) (2017) 219–231, https://doi.org/10.1016/j.tibs.2016.10.008.